Experimental Study of Magnetic Reconnection in Partially Ionized Plasmas Using Rotating Magnetic Field*)

Yoshifumi TAKAHATA, Ryoma YANAI and Michiaki INOMOTO[1)]

Graduate School of Engineering, The University of Tokyo, Bunkyo, Tokyo 113-0032, Japan
[1)]*Graduate School of Frontier Science, The University of Tokyo, Kashiwa, Chiba 277-8561, Japan*

(Received 27 December 2018 / Accepted 31 January 2019)

Experimental setup to achieve long-pulse magnetic reconnection in partially ionized plasmas was developed using the rotating magnetic field technique. Two field-reversed configuration plasmas were formed and sustained along the axial direction in the experimental vessel, and the quasi-steady magnetic reconnection condition with the ionization degree of the order of 1 % was maintained for more than 20 ms between the plasmas. Time duration of magnetic reconnection longer than the ion-neutral collision time and plasma parameters where the neutral particles possibly affect the reconnection process, were achieved. Reconnection events observed under the present experimental conditions were classified into three cases according to the ionization degree, and a new experimental regime for magnetic reconnection in partially ionized plasmas was successfully demonstrated.

Keywords: magnetic reconnection, rotating magnetic field, partially ionized plasmas, ambipolar diffusion

DOI: 10.1585/pfr.14.3401054

1. Introduction

Magnetic reconnection is a phenomenon that changes the global magnetic topology and converts magnetic energy into kinetic energy of magnetized plasmas by reconnecting of anti-parallel magnetic field lines in localized diffusion region [1]. Although magnetic reconnection is a local phenomenon, it can change the global geometry of magnetic field. This phenomenon is studied or observed in a range of solar corona, magnetosphere, laboratory plasmas, numerical simulations and so on. Since reconnection is a universal phenomenon covering a wide range of plasmas, its physical behavior can be changed drastically by parameters such as the topology of magnetic field, plasma density, degree of ionization, plasma temperature and so on.

Magnetic reconnection is also observed in partially ionized plasmas such as the solar chromosphere [2], and attracts attention because reconnection in the solar chromosphere is a candidate for a coronal heating source [3]. In partially ionized plasmas, the behavior of magnetic reconnection is predicted to be different from fully ionized plasmas because of the interaction between plasmas and neutral particles, known as the "ambipolar diffusion" effect in solar physics. Magnetic reconnection in partially ionized plasmas has been numerically investigated [4, 5], and a high reconnection rate due to plasmoid instability and the effect of neutral particles is suggested. Although closed-type laboratory experiments have been conducted [6], the ambipolar diffusion effect has not been clearly observed because of the limited discharge periods insufficient to achieve flowing neutral particles dragged by ions. Since closed-type reconnection experimental devices utilize inductive plasma breakdown, discharge periods are limited. Thus, another experimental approach including the quasi-steady state is required to testify the effect of neutral particles in magnetic reconnection.

We have successfully developed a new experimental scheme to achieve long-pulse magnetic reconnection by using the rotating magnetic field (RMF) technique [7]. In this paper, we report experimental results of long pulsed magnetic reconnection with sufficient plasma parameters to investigate the effect of neutral particles on magnetic reconnection.

2. Experimental Setup

Field-reversed configuration (FRC) is a magnetic field configuration for plasma confinement characterized by its simple topology composed of poloidal magnetic surfaces without toroidal magnetic field B_t [8]. Since β in FRC plasma is extremely high, it is expected and studied as an advanced fuel fusion reactor.

RMF technique is used for creating and sustaining FRC plasmas [9–12]. By applying transverse magnetic field rotating in the azimuthal direction with frequency much higher than the ion cyclotron frequency and much lower than the electron cyclotron frequency, only electrons can keep up with the variation of magnetic field, and azimuthal electron current is driven. This net DC toroidal plasma current creates poloidal magnetic field and finally

author's e-mail: ytakahata@ts.t.u-tokyo.ac.jp
*) This article is based on the presentation at the 27th International Toki Conference (ITC27) & the 13th Asia Pacific Plasma Theory Conference (APPTC2018).

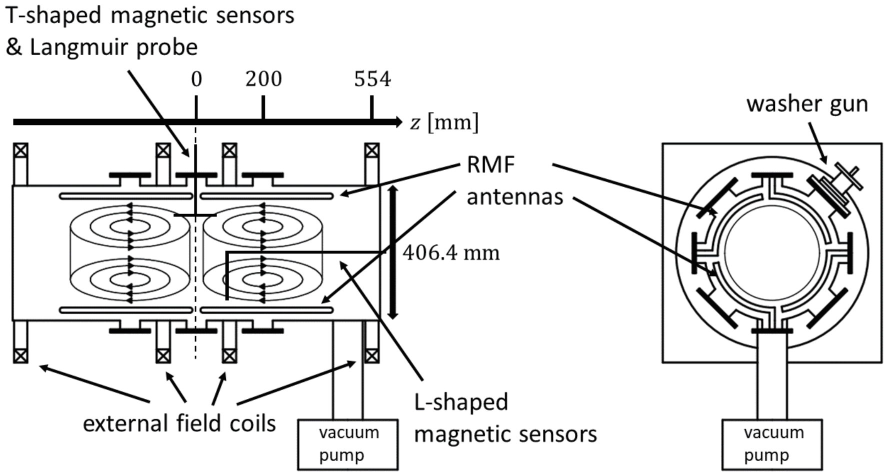

Fig. 1 Schematic view of the experimental device. Axial cross section (left) and radial cross section (right). Four 9-turn RMF antennas are installed on the left and right inside the vessel. Magnetic reconnection occurs on the midplane (z = 0 m), between the two FRC plasmas formed by RMF.

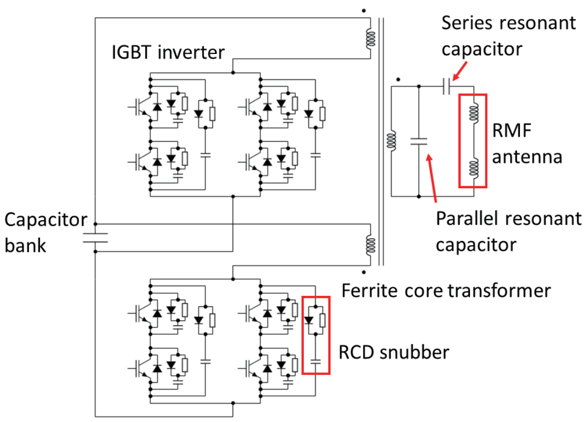

Fig. 2 Circuit diagram of the RMF power supply circuit composed of a capacitor bank, a push-pull inverter circuit, a ferrite core transformers, and a series resonant circuit.

forms FRC's closed magnetic surfaces surrounded by open magnetic field created by external coils.

Figure 1 shows a schematic view of the experimental device. The device has a cylindrical vessel made of stainless steel with 0.40 m diameter and 1.1 m length. To create and sustain FRC plasmas, two sets of four 9-turn RMF antennas are installed and azimuthally arrayed inside the vessel. Antennas are located at r = 0.16 m with axial length of 0.40 m. Push-pull inverter circuits employing an insulated gate bipolar transistor (IGBT) and series resonant circuits are installed as a power supply, as shown in Fig. 2. Maximum antenna current is 100 A and the applied RMF is about 15 G without plasma on the geometrical axis. The RMF frequency is 102 kHz, which is higher than the ion cyclotron frequency f_{ci} (6 kHz in case of helium) and lower than the electron cyclotron frequency f_{ce} (42 MHz). Four 100-turn coils are installed outside the vessel to form external axial field. Preionized helium gas is supplied through the washer gun mounted on the radial port (see Fig. 1). Neutral gas pressure during discharge is controlled within 0.1 - 100 mTorr, and the typical vacuum pressure is 7.5×10^{-6} Torr.

In this experiment, the two FRC plasmas aligned along the axial direction are created and sustained by odd-parity RMF [13]. These plasmas cause magnetic reconnection on the midplane of the vessel (z = 0 m) by contacting the anti-parallel poloidal magnetic fields of the two FRC plasmas.

Two-dimensional (2D) profiles of magnetic fields are measured by magnetic probes using Hall effect magnetic sensors. The L-shaped probe is composed of 14×2 Hall sensors that measure the radial profiles of axial and toroidal magnetic fields B_z and B_t with 1 cm spacing. The T-shaped probe is composed of 15 Hall sensors that measure the axial profile of reconnecting magnetic field B_r across the current layer with 1 cm spacing. These probes are scanned in the axial and the radial direction to obtain the 2D profiles of magnetic fields assuming reproducibility between discharges. These data are used to calculate toroidal current densities $J_t = (\partial B_r/\partial z - \partial B_z/\partial r)/\mu_0$, and radial and axial current density $J_r = -(\partial B_t/\partial z)/\mu_0$ and $J_z = [\partial(rB_t)/\partial r]/\mu_0 r$ assuming axisymmetry. Langmuir probe is inserted at the midplane of the vessel. Radial distribution of electron temperature T_e and electron density n_e are measured using a triple Langmuir probe method, and floating plasma potential V_f is also measured. Neutral gas pressure is measured using a Baratron vacuum gage. Typical plasma parameters are as follows: maximum axial field reversal caused by the plasma current $\Delta B_z \sim 25$ G, $n_e \sim 1 \times 10^{18}$ m^{-3}, and $T_e \sim 6$ eV.

3. Results and Discussions

By applying the left-side RMF in Fig. 1, a single RMF-FRC plasma was sustained for more than 15 ms.

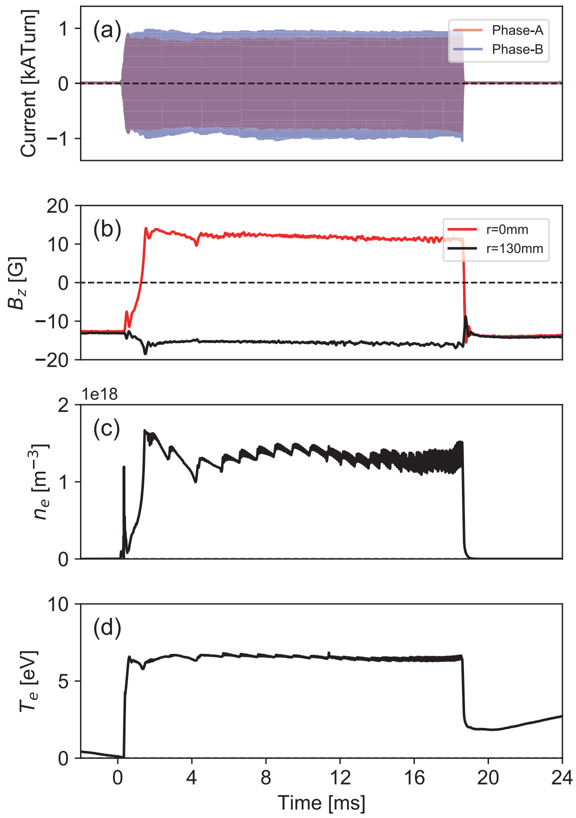

Fig. 3 Time evolution of (a) RMF antenna current, (b) axial magnetic field B_z at $r = 0$ mm and $r = 130$ mm, $z = -200$ mm, (c) electron density n_e at $r = 50$ mm, $z = -200$ mm, (d) electron temperature T_e at $r = 50$ mm, $z = -200$ mm in the case of helium discharge with the fill-gas pressure of 0.6 mTorr.

Time evolution of the plasma parameters are shown in Fig. 3. In this discharge, helium gas was filled from −25 to −23 ms with the fill-gas pressure of 0.6 mTorr, and plasma breakdown occurred at 0.3 ms simultaneously with the discharge of the washer gun preionization. The charged voltage of the capacitor bank of the RMF power supply was 500 V, and the duty ratios of the IGBTs were changed with time passage to keep the antenna current constant (∼1 kATurn) during the discharge. Before the antenna current was supplied, the steady axial magnetic field of $B_{ez} \sim -12$ G was formed by the external field coils. The axial magnetic field on the axis ($r = 0$ mm) gradually increased and finally reached $B_z \sim 12$ G created by the plasma current driven by RMF (see Fig. 3 (b)). Thus, FRC plasma with closed flux surfaces was created and sustained. The electron density was $n_e \sim 1 \times 10^{18}$ m^{-3} and the electron temperature was 6 eV at the center of plasma.

Based on the result of a single FRC plasma formation and sustainment, the two FRC plasmas were sustained to induce magnetic reconnection. The effect of neutral particles on magnetic reconnection was experimentally investigated by varying the fill-gas pressure of helium. The fill-gas pressure was within 0.3 - 9.0 mTorr, and the ionization degree was in the order of 1 %. Profiles of poloidal magnetic field and toroidal current density derived from the magnetic sensor signals in the case of the ionization degree of 2.0 % are shown in Fig. 4. Two closed private magnetic surfaces of the FRC plasmas were formed by RMF side-by-side along the axial direction, and the common magnetic flux was created by the reconnection of these private magnetic surfaces. In contrast to ordinary RMF-FRC plasmas where the positive toroidal current (red color in Fig. 4) is driven, the reversed current layer (blue color in Fig. 4) was observed around the midplane of the vessel. Figure 5 shows the time evolution of the toroidal current density at three locations. Negative toroidal current was induced at the reconnection point (blue), whereas the current at the upstream region (red) was positive. The reversed current layer was steadily maintained when the external magnetic field profile was adequately adjusted, suggesting the occurrence of steady magnetic reconnection between the two FRC plasmas.

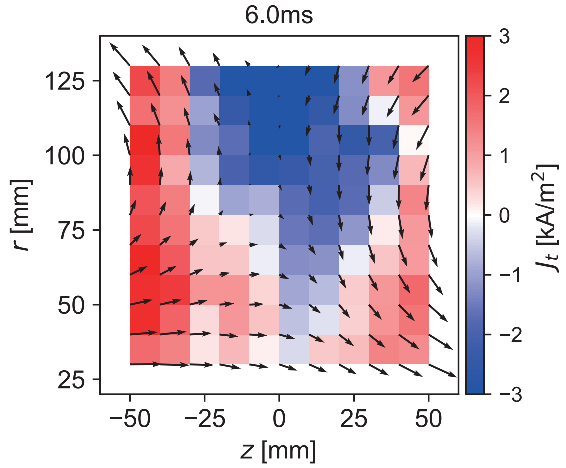

Fig. 4 Profiles of poloidal magnetic field and toroidal current density derived from magnetic sensor signals. Arrows show the strength and direction of magnetic field, and color shows toroidal current density. In contrast to ordinary RMF-FRC plasmas, the reversed current layer was steadily observed around the midplane ($z = 0$ m).

The ion-neutral collision time $\tau_{in} = 1/\nu_{in} \sim 10$ - 200 µs where ν_{in} is the collision frequency between ion and neutral particles, was sufficiently shorter than the estimated reconnection time $\tau_{rec} = L/0.1v_A \sim 3$ - 15 ms for the typical scale length L of 0.1 m and the total mass Alfvén velocity $v_A = B/\sqrt{\mu_0 (m_i n_i + m_n n_n)}$ of 60 - 300 m/s. A plasma lifetime of 20 ms was long enough to investigate the effect of the interaction between ion and neutral particles. Ignoring the inertia and the pressure terms, the induction equation of magnetic field in partially ionized plasmas can be represented as follows:

$$\frac{\partial \boldsymbol{B}}{\partial t} = \nabla\times\left(\boldsymbol{U}_n \times \boldsymbol{B} - \eta \boldsymbol{J} - \frac{\boldsymbol{J}\times\boldsymbol{B}}{e n_e} + \frac{(\boldsymbol{J}\times\boldsymbol{B})\times\boldsymbol{B}}{\nu_{in} m_i n_i}\right), \tag{1}$$

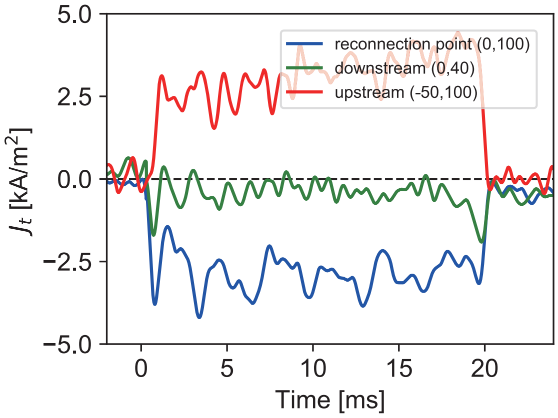

Fig. 5 Time evolution of toroidal current density J_t at the upstream region (red), downstream region (green), and reconnection point (blue). Negative current was maintained for 20 ms at the reconnection point.

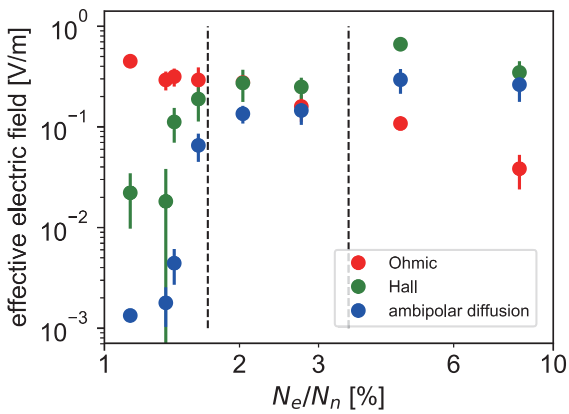

Fig. 6 Dependencies of the toroidal components of the Ohmic term $-\eta J_t$, the Hall term $-(\boldsymbol{J}\times\boldsymbol{B}/en_e)_t$, and the ambipolar diffusion term $[(\boldsymbol{J}\times\boldsymbol{B})\times\boldsymbol{B}/\nu_{in}m_in_i]_t$ of the induction equation inside the current layer (r = 100 mm, z = 20 mm) on ionization degree.

where $\eta\boldsymbol{J}$ is the Ohmic term caused by collision between electron and ion or neutral particles, and $\boldsymbol{J}\times\boldsymbol{B}/en_e$ is the Hall term. The effect of the interaction between ion and neutral particles brings about the ambipolar diffusion term $(\boldsymbol{J}\times\boldsymbol{B})\times\boldsymbol{B}/\nu_{in}m_in_i$. This term arises from the relative flow velocity $(\boldsymbol{J}\times\boldsymbol{B})/\nu_{in}m_in_i$, between ion fluid and neutral fluid dragged by ions. Thus, the ion-neutral collision frequency must be set within the intermediate range to achieve the compatible condition for a large relative velocity and a sufficient drag. Three terms in the induction equation were evaluated using three components of magnetic field and current density derived from the magnetic sensor signals, and electron density obtained from the triple Langmuir probe. Dependencies of the toroidal components of the three terms of the induction equation inside the current layer (r = 100 mm, z = 20 mm) on ionization degree are shown in Fig. 6. Error bars represent the standard deviation of the variation in time. The Ohmic term decreased

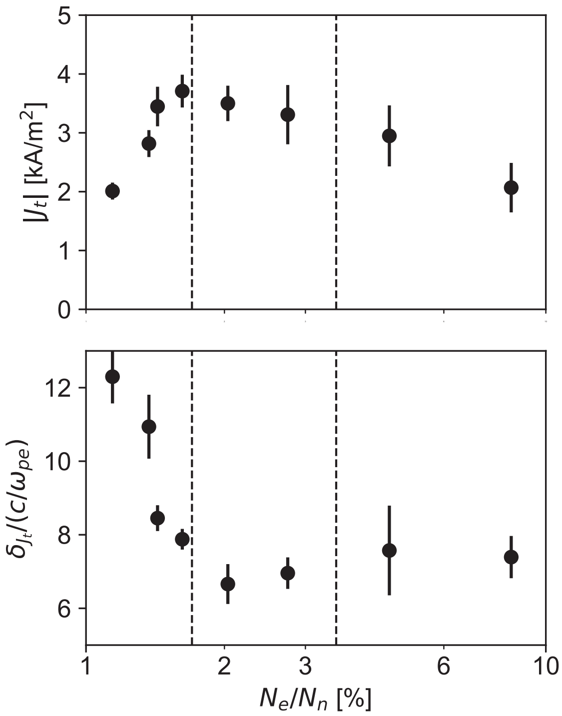

Fig. 7 Dependencies of maximum toroidal reversed current density (top), and the current sheet thickness normalized to electron skin depth (bottom) on ionization degree.

with the ionization degree because neutral particle density decreased with the ionization degree, thereby decreasing the collision frequency between electron and neutral particles. Contrary to the Ohmic term, the ambipolar diffusion term increased with the ionization degree. This is because the collision frequency between ion and neutral particles decreased with the ionization degree. When the ionization degree exceeded 2 %, the ambipolar diffusion term was of the same order as the Ohmic and the Hall terms. The conditions of time duration and plasma parameters required for observing the effect of neutral particles in magnetic reconnection were achieved. We should note that Lundquist number $S = \mu_0 v_A L/\eta$ was in the order of 0.01 – 1 which is much smaller than that of the chromosphere plasma 10^6 - 10^8 with scale length of $L \sim 1\times10^6$ m [5], and was insufficient for the effect of the microstructure like plasmoid to be observed [14].

The reconnection events in this experiment can be classified into three cases based on ionization degree; the high ionization degree case where the Hall and the ambipolar diffusion terms are dominant, the low ionization degree case where the Ohmic term is dominant, and the middle ionization degree case where the three terms are of the same order. In the high ionization regime, the mean free path of ion-neutral collision $\lambda_{in} = v_{ti}/\nu_{in}$ where v_{ti} is ion thermal velocity, was longer than the scale length L, hence the interaction between ion and neutral particles was considered not to affect the reconnection process.

Figure 7 shows the dependencies of the maximum toroidal reconnection current density and the current sheet thickness normalized to electron skin depth $d_e = c/\omega_{pe}$ on ionization degree. The current sheet thickness is derived from the magnetic sensor signals from the T-shaped probe fitted to the Harris sheet $B_r = B_{rec} \tanh((z - z_0)/\delta_{J_t})$. Error bars represent the standard deviation of the variation in time. In the low ionization case where the Ohmic term dominates the induction equation, the current sheet thickness decreased with increasing the ionization degree and reached $\delta_{J_t} \sim 7c/\omega_{pe}$, together with the increment in the current density which compensates for the reduction of the resistivity and reconnection electric field.

The normalized current sheet thickness was almost constant in the middle and high ionization cases where the Hall and the ambipolar diffusion terms became dominant. The current density showed a gradually decreasing trend in these regimes, which is qualitatively similar to previously reported results [6]. However, magnetic reconnection in the middle and the high ionization degree showed similar magnetic structure and the effect of neutral particles was not observed clearly in this experiment. Since the ratio of the ambipolar diffusion term to the Hall term is proportional to B/n_n, increment of reconnection magnetic field, which requires upgrading the RMF power supply, is needed to achieve the condition where only the ambipolar diffusion term dominates the induction equation.

4. Summary

Magnetic reconnection in partially ionized plasmas was experimentally investigated using the RMF technique. The two FRC plasmas were formed along the axial direction and quasi-steady magnetic reconnection was induced by contacting their poloidal fluxes. The time duration of reconnection of 20 ms was sufficiently long compared with the ion-neutral collision time, and the ambipolar diffusion term in the induction equation was sufficiently large. By varying the ionization degree, reconnection events in this experiment were classified into three cases. These three cases possibly reflect the Hall effect, the interaction between ion and neutral particles, and the Ohmic diffusion respectively, and a new experimental regime for magnetic reconnection in partially ionized plasmas was successfully demonstrated. However, the effect of neutral particles was not clearly observed under the present experimental conditions, and the RMF power supply must be improved to achieve larger reconnection field and more significant neutral particle effect.

Acknowledgements

This work was supported by Grant-in Aid for Scientific Research (KAKENHI) Nos. 26287143, 23654200, 22686085 and NIFS Collaboration Research Program Nos. NIFS17KNWP006, NIFS14KNWP004.

[1] M. Yamada, R. Kulsrud and H. Ji, Rev. Mod. Phys. **82**, 603 (2010).
[2] N. Nishizuka, M. Shimizu, T. Nakamura, K. Otsuji, T.J. Okamoto, Y. Katsukawa and K. Shibata, Astrophys. J. **683**, L83 (2008).
[3] P.A. Sturrock, Astrophys. J. **521**, 451 (1999).
[4] J.E. Leake, V.S. Lukin and M.G. Linton, Phys. Plasmas **20**, 061202 (2013).
[5] L. Ni, B. Kliem, J. Lin and N. Wu, Astrophys. J. **799**, 79 (2015).
[6] E.E. Lawrence, H. Ji, M. Yamada and J. Yoo, Phys. Rev. Lett. **110**, 015001 (2013).
[7] R. Yanai, Y. Takahata and M. Inomoto, Rev. Sci. Instrum. **89**, 103506 (2018).
[8] L.C. Steinhauer, Phys. Plasmas **18**, 070501 (2011).
[9] I.R. Jones, Phys. Plasmas **6**, 1950 (1999).
[10] H.Y. Guo, A.L. Hoffman, R.D. Milroy, L.C. Steinhauer, R.D. Brooks, C.L. Deards, J.A. Grossnickle, P. Melnik, K.E. Miller and G.C. Vlases, Phys. Plasmas **15**, 056101 (2008).
[11] S.A. Cohen, B. Berlinger, C. Brunkhorst, A. Brooks, N. Ferraro, D.P. Lundberg, A. Roach and A.H. Glasser, Phys. Rev. Lett. **98**, 145002 (2007).
[12] M. Inomoto, K. Kitano and S. Okada, Phys. Rev. Lett. **99**, 175003 (2007).
[13] S.A. Cohen and R.D. Milroy, Phys. Plasmas **7**, 2539 (2000).
[14] H. Ji and W. Daughton, Phys. Plasmas **18**, 111207 (2011).